1998

Integrable Unsteady Motion With an Application to Ocean Eddies

A. D. Kirwan Jr.

Bruce L. Lipphardt

Original Publication Citation

Kirwan, A. D., & Lipphardt, B. L. (1998). Integrable unsteady motion with an application to ocean eddies. *Nonlinear Processes in Geophysics, 5*(3), 145-151.

Integrable unsteady motion with an application to ocean eddies

A. D. Kirwan, Jr., B. L. Lipphardt, Jr.

Nonlinear Processes in Geophysics (1998) 5: 145–151

Nonlinear Processes in Geophysics

Integrable unsteady motion with an application to ocean eddies

A. D. Kirwan, Jr. and B. L. Lipphardt, Jr.

Center for Coastal Physical Oceanography, Old Dominion University, Norfolk, VA 23529, USA

Received: 25 November 1998 – Accepted: 26 March 1999

Abstract. Application of the Brown–Samelson theorem, which shows that particle motion is integrable in a class of vorticity–conserving, two–dimensional incompressible flows, is extended here to a class of explicit time dependent dynamically balanced flows in multi–layered systems. Particle motion for nonsteady two–dimensional flows with discontinuities in the vorticity or potential vorticity fields (modon solutions) is shown to be integrable. An example of a two–layer modon solution constrained by observations of a Gulf Stream ring system is discussed.

1 Introduction

Recently, Brown and Samelson (1994) showed that particle motion is integrable in any vorticity–conserving, two–dimensional incompressible flow if the vorticity is a differentiable function with a non–zero gradient. Their proof did not make explicit use of any functional relation between vorticity and the streamfunction and so this result applies to any flow that has a Lagrangian constant of motion. Applicability to nonsteady dynamically balanced flows is unknown since only kinematically prescribed flows were cited.

The purpose of this communication is to show that the Brown–Samelson result applies to a class of explicit time dependent dynamically balanced stratified flows of some interest to atmospheric scientists and oceanographers. These solutions satisfy the potential vorticity equations for layered fluids in which the potential vorticity may even be discontinuous. One solution form, the rotating modon, can be developed analytically, but application of patch conditions at solution boundaries results in an eigenvalue problem that is most readily solved numerically.

Here, we demonstrate that this class of solutions is integrable, a property of these solutions that was previously unknown. To our knowledge, the rotating modon solution is the first nontrivial example of a two–dimensional, nonsteady, incompressible vortical flow with integrable particle motions. Demonstration of the integrability of these solutions represents an important extention of the Brown–Samelson theorem to a class of multi–layered flows that are in dynamical balance.

The theory is developed in the next section while section 3 presents an application of the baroclinic rotating modon model to observations of Gulf Stream ring 82B. A synopsis and suggestions for further research are given in the final section.

2 Theory

The starting point for the analysis is Ertel's potential vorticity theorem for an N–layered system:

$$\partial q_j/\partial t + J(\psi_j, q_j) = S_j \ , \ j = 1, ...N. \qquad (1)$$

Here q_j and ψ_j are the potential vorticity and streamfunction for layer j, J is the Jacobian operator and S_j represent non–conservative effects. They are included here only to allow for the possibility of discontinuous q_j fields. For geophysical fluid dynamics, the q_j and ψ_j are related by

$$q_j = \nabla^2\psi_j - \sum_{k=1}^{N} F_{jk}\psi_k \qquad (2)$$

where F_{jk} are layer Froude numbers. The Brown–Samelson result was obtained for the case $N = 1$, $F_{jk} = S_j = 0$ but does not depend on a specific functional relation between vorticity and streamfunction, such as Eq. (2).

The key issue in applying the Brown–Samelson theorem is to find Lagrangian motion constants for each layer. These constants then constitute the Hamiltonians for a canonical system. Here we consider swirling

Correspondence to: A. D. Kirwan, Jr.

flows in a circular coordinate system and seek solutions to (1) of the general form

$$\psi_j\,(r,\theta,t) = M_j\,[r, n\,(\theta - \omega t)]\,. \tag{3}$$

Here, the M_j are smooth, n is any positive integer, and the subscript refers to layer j.

For the conditions just stated, the candidate Hamiltonians are functionals of $\psi_j - \omega r^2/2$ or

$$H_j = H_j(\psi_j - \omega r^2/2 + Q_j). \tag{4}$$

The constants Q_j in Eq. (4) identify the strength of the vortex system centered at $r = 0$.

To show that Eq. (4) satisfies the conservative form of Eq. (1), note that from Eq. (3)

$$\partial/\partial t = -\omega\,\partial/\partial\theta. \tag{5}$$

Then

$$\partial H_j/\partial t + J(\psi_j, H_j) = J(H_j, H_j) \equiv 0. \tag{6}$$

The flow produced by Eq. (4) arrests the steady rotation in physical space produced by Eq. (3). Since these Hamiltonians make no explicit use of any dependency on vorticity they extend the Brown–Samelson result to baroclinic flows.

Are there any nontrivial solutions to realistic flows that have Eq. (4) as Hamiltonians? One class of solutions to Eq. (1) are rotating modons. A barotropic solution was reported by Mied *et al.* (1992) and applied to Gulf Stream rings by Hooker *et al.* (1995). Lipphardt (1995) applied a baroclinic theory to Gulf Stream rings. A detailed analysis of the baroclinic theory including effects of local bottom topography is given in Kirwan *et al.* (1997).

Rotating modons are weak or generalized solutions in which the potential vorticity (q_j) and streamfunction (ψ_j) are of the form

$$q_j = \Gamma_j(H_j)\sigma(r_j - r) \tag{7}$$

$$\psi_j = G_j(r) + B_j^p(r)e^{i[n(\theta-\omega t)]}. \tag{8}$$

In Eq. (7) $\sigma(r_j - r)$ is the Heaviside function and the Γ_j are smooth but otherwise arbitrary functionals.

Physically these solutions superpose axisymmetric vortices G_j and n azimuthally paired vortices ($2\,n$ vortices in all) with radial structure given by B_j^p, where p is the radial mode number. For the barotropic and baroclinic rotating modons discussed below, the B_j^p are either Bessel functions, or polynomials. The fluid in each layer is rotating with the same angular velocity ω. The azimuthal mode number n is also the same for each layer; however, the strength of the axisymmetric vortices G_j may mask the modal structure in some layers. Translating rectilinear modons are Galilean invariant but steady rotating flows such as those given by Eq. (3) are not. This fact contributes to interesting differences between the two classes of flows as discussed by Kirwan *et al.* (1997). Note that if $\Gamma_j\ |_{r=r_j} \neq 0$, then there will be a discontinuity in q_j at the modon boundaries r_j. Of course, ψ_j and $\nabla\psi_j$ must be continuous everywhere.

Substitution of Eq. (7) and Eq. (8) into Eq. (1) yields, after some calculation that uses Eq. (5) and the generalized derivative of σ,

$$J(H_j, \Gamma(H_j))\sigma(r_j - r) + (1/r)\Gamma_j(H_j)(\partial H_j/\partial\theta)\delta(r_j - r) = S_j \tag{9}$$

where δ is the delta function. Since $J(H_j, \Gamma(H_j)) \equiv 0$, Eq. (8) identifies the structure of the non-conservative terms S_j. They are non-zero only at the modon boundaries. In the special case $S_j = 0$ there are no modon boundaries and Eq. (1) simply becomes the baroclinic extension of the Brown–Samelson theorem. Since the S_j play no role in the solution for ψ_j they are not considered further.

It might be noted that integrability of particle motion in flows of the form Eq. (3) is not obvious. For example, Brown (1998) investigated different solutions to Eq. (1) for the case $N = 2$ but with the lower layer in hydrostatic balance (the reduced gravity case) and found chaos.

Solutions such as Eq. (7) that are discontinuous are called weak solutions. As noted by Whitham (1974, page 26), such solutions usually signal a breakdown of physical approximations, and repair of these breakdowns must proceed in step with the development of strong solutions. Investigation of these strong solutions is not attempted here, however.

As discussed by Kirwan *et al.* (1997) rotating modon solutions differ from their conventional rectilinear translating modon cousins in that the former may have discontinuities in the vorticity field at the modon boundaries while the latter have the flexibility to prescribe modon boundaries as streamlines. One reason for this difference is the requirement that the streamfunction for rotating modon solutions vanish at infinity while rectilinear modons usually have an imposed large scale shear field or a beta effect at infinity. Such conditions provide sufficient flexibility to impose additional constraints that modon boundaries also be streamlines.

The possibility of developing rotating modon solutions that also have streamline boundaries is not explored here principally because we consider discontinuous vorticity fields as the more general condition and thus the more stringent test of the Brown–Samelson result. Note, however, that "shock" solutions to the planetary scale geostrophic equations are not unknown. For example Nof (1986) and Dewar (1987, 1991, and 1992) have found solutions in which large changes in potential vorticity developed across the shock even when momentum and energy were conserved.

Equations (2) and (7) are to be solved for ψ_j. To see the structure of the differential equations, the layer number will correspond to the rank of the layer's modon radius r_j (not to its serial position in the water column) so that (r_1, r_N) refer to the layer with the (least, largest) modon radii in an N–layered ocean, not the top and bottom layers.

For $r > r_N$ the ψ_j satisfy the system of Helmholtz equations

$$\nabla^2\psi_j - \sum_{k=1}^{N} F_{jk}\psi_k = 0. \qquad (10)$$

In the annulus $r_{N-1} < r < r_N$, the ψ_j satisfy

$$\nabla^2\psi_j - \sum_{k=1}^{N} F_{jk}\psi_k = 0\ ,\ i = 1, ...N-1$$

$$\nabla^2\psi_N - \sum_{k=1}^{N} F_{Nk}\psi_k = \Gamma_N(\psi_N - \omega r^2/2 + Q_N). \qquad (11)$$

For the innermost annulus, $r < r_1$, the ψ_j satisfy

$$\nabla^2\psi_j - \sum_{k=1}^{N} F_{jk}\psi_k = \Gamma_j(\psi_j - \omega r^2/2 + Q_j). \qquad (12)$$

For Γ_j that are linear in their arguments, the system of Eq. (10) through Eq. (12) comprises a system of linear inhomogeneous coupled Helmholtz equations.

The solutions at each of the boundaries r_j also must satisfy the patch conditions

$$\lim_{r\to r_j^-}(\psi_j, \nabla\psi_j) = \lim_{r\to r_j^+}(\psi_j, \nabla\psi_j) \qquad (13)$$

as well as the existence and asymptotic conditions

$$\lim_{r\to 0} \mid \psi_j \mid < \infty \qquad (14)$$

$$\lim_{r\to\infty} \psi_j \to 0. \qquad (15)$$

Application of Eq. (13) through Eq. (15) to the solutions obtained from Eq. (10) through Eq. (12) produces an eigenvalue problem whose roots determine the number of radial modes. See Kirwan *et al.* (1997) for details. If there are no modon boundaries then the problem reduces to solving Eq. (12) subject to Eq. (14) and Eq. (15).

As shown by Stern (1975) and Flierl *et al.* (1980) it is possible to require continuity of ψ_j and $\nabla\psi_j$ at the modon boundaries as well as to require the boundaries to be streamlines in the translating modon case. However, in the present case it is noted that Eq. (12) is not sufficient to ensure the last condition. Thus particles may cross potential vorticity discontinuities; or, as stated by Eq. (7), q_j is a discontinuous function of H_j if $\Gamma_j \mid_{r=r_j} \neq 0$. In the spirit of Whitham (1974) the discontinuities should be viewed as the inviscid approximation to small but finite boundary layers.

Table 1. Parameter values used to simulate the WCR 82B system

Environmental parameters	
Upper layer mean thickness	777 m
Lower layer mean thickness	1923 m
Reduced gravity	0.0106 m s^{-2}
Coriolis acceleration	9.175 x 10^{-5} rad s^{-1}
Geometric parameters	
Azimuthal mode number	1
Upper layer radial mode number	1
Lower layer radial mode number	1
Upper layer modon radius	75 km
Lower layer modon radius	130 km
Arbitrary amplitudes	
Region I barotropic mode amplitude	1.2227 x 10^{-2}
Upper layer axisymmetric rider	-8.000 x 10^{-4}
Lower layer axisymmetric rider	-3.235 x 10^{-2}

3 Application to Gulf Stream Ring 82B

Here we present an application of the rotating baroclinic modon solution to perhaps the best documented ring in oceanography, Gulf Stream ring 82B. It was the second ring shed by the Gulf Stream in 1982 and was the subject of an extensive observational effort. Joyce (1985) provides an overview of this program and Joyce and Kennelly (1985) give a detailed picture of the near surface velocity field during a portion of the field program. More recently Holdzkom *et al.* (1995) have shown that for much of its existence 82B was accompanied by a small intense cyclonic structure.

We follow the analysis of Lipphardt (1995) and treat this dipolar structure as a two layered rotating modon. In this case there are 12 solution parameters. By appealing to remote sensing observations and plausible physical arguments Lipphardt (1995) was able to fix 9 of these parameters and then tuned the remaining 3 by a sensitivity study so they provided a best fit to the observations. The adjusted parameters were the lower layer modon radius, the strength of the upper layer rider and the amplitude of the upper layer azimuthal mode. All parameter values used in the calculations below are displayed in Table 1.

Figure 1 shows three examples of particle trajectories for three complete modon rotations for the baroclinic modon simulation of WCR 82B, using the modon parameters shown in Table 1. In each panel, trajectories in the fixed reference frame (shown in red) and trajectories in a frame that rotates with the modon (shown in blue) are overlaid on contours of the upper layer Hamiltonian from Eq. (4). The particle's initial position is

shown by a black diamond. Since the Hamiltonian field contains two saddle points, a uniform contour interval could not be used effectively in the panels of Fig. 1. Instead, the following details describe the contour scheme for representing the Hamiltonian:

- The axes of the modon coordinate system are shown as dot–dashed lines. The modon rotates clockwise about the origin, where these two lines cross.
- The dotted circle, centered on the origin, defines the upper layer modon radius (75 km).
- The three solid black circles show the three stagnation points in the Hamiltonian field. The stagnation point below the origin corresponds to the center of the cyclone. The first stagnation point above the origin corresponds to the anticyclone center. The second stagnation point above the origin lies outside the upper layer modon boundary.
- The two solid black squares show the two saddle points in the Hamiltonian field.
- The heavy solid black contour value is 7.042×10^7 $cm^2\ s^{-1}$, the approximate saddle point value.
- Inside the saddle point contour, and moving outward from the cyclone center, the Hamiltonian is increasing, and the contour levels are (-8.0×10^7, -4.0×10^7, 4.0×10^7) $cm^2\ s^{-1}$. Negative contours are shown as dotted lines.
- Inside the saddle point contour, and moving outward from the anticyclone center, the Hamiltonian is decreasing, and the contour levels are (1.5×10^8, 1.0×10^8) $cm^2\ s^{-1}$.
- Outside the saddle point contour, and moving outward, the Hamiltonian is increasing and the contour levels are (1.0×10^8, 1.5×10^8, 3.0×10^8) $cm^2\ s^{-1}$.

The upper panel of Fig. 1 shows a particle that is initially positioned just inside the modon boundary and remains inside the modon boundary throughout the three modon rotations. The middle panel of Fig. 1 shows a particle that is initially positioned just outside the modon boundary, but crosses the boundary several times over three modon rotations. The lower panel of Fig. 1 shows a particle that is initially positioned well outside the modon boundary, and remains outside the boundary throughout the three modon rotations. The reason that the fixed reference frame trajectories (in red) can be so complicated is that the particle orbit periods are generally not commensurate with the modon rotation period, so that the particle paths and the Hamiltonian field are usually out of phase.

Figure 2 shows a time series of the evolution of a blob of 2000 particles, randomly positioned inside a 10 km circle initially positioned at the saddle point in the upper

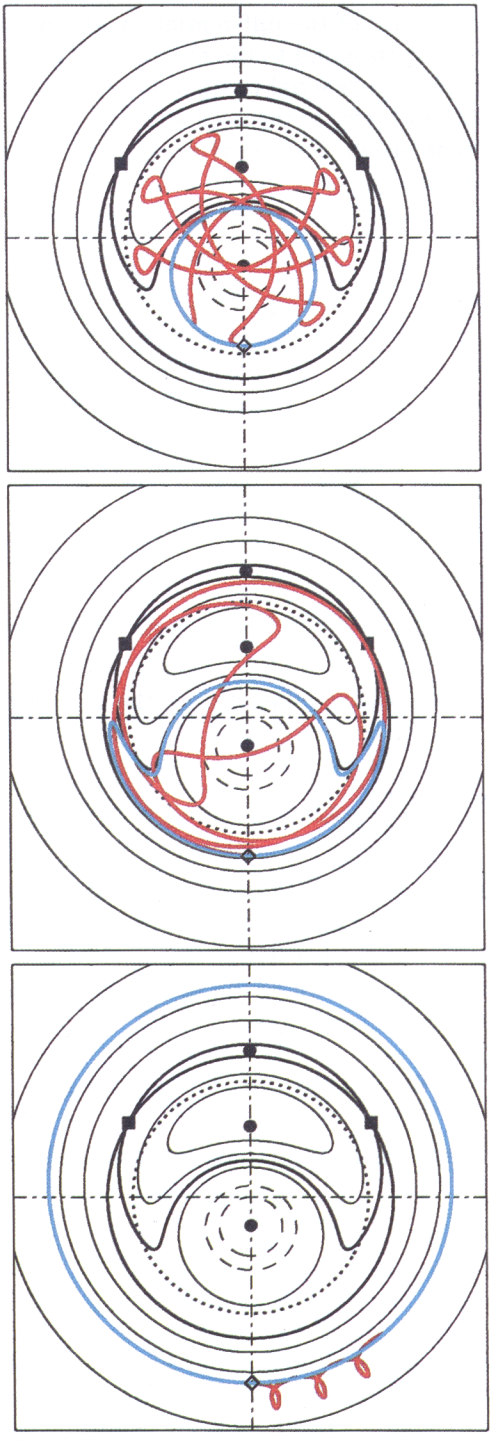

Fig. 1. Particle trajectories overlaid on contours of the upper layer Hamiltonian for three complete modon rotations for the baroclinic modon simulation of WCR 82B. Red trajectories are referenced to a fixed reference frame, while blue trajectories are referenced to a frame that rotates with the modon. The upper panel shows a particle initially inside the modon that remains there. The middle panel shows a particle initially outside the modon that crosses the modon boundary several times. The lower panel shows a particle initially outside the modon boundary that remains there. A description of the Hamiltonian contours is contained in the text.

right quadrant. In each panel in Fig. 2, groups of particle positions are overlaid on a contour plot of the upper layer Hamiltonian. The contour plots are constructed in the same way as those in Fig. 1. Particles shown in blue were initially positioned at a radius greater than the saddle point radius. Red particles were initially positioned at a radius less than or equal to that of the saddle point. In each panel, the time (in modon rotation periods) is shown at the lower right. Figure 2 shows that, near the saddle points, a great deal of mixing occurs over one modon rotation, with the saddle point defining a mixing boundary. Particles initially outside the saddle point stay there and end up scattered around the outer perimeter of the dipole. Particles initially inside the saddle point remain inside, and are readily advected by the high velocities around the periphery of the anticyclone. In addition, note that many of the red particles cross the modon boundary, where a discontinuity in vorticity exists.

A plot of particle positions, strobed at the modon rotation period over many periods, provides further insight into the integrability of this flow. As evident from Eq. (4) and Eq. (6), particles will follow paths of constant Hamiltonian value in the frame that rotates with the modon. The Poincaré section, then, will show particle positions coinciding with contours of the Hamiltonian. Figure 3 shows the evolution of the Poincaré sections for the three particle trajectories shown in Fig. 1. The Poincaré sections are overlaid on contours of the upper layer Hamiltonian, constructed as in Fig. 1. Poincaré sections for the particle trajectory shown in the (upper, middle, lower) panel of Fig. 1 are shown in (red, green, blue). The evolution time, in modon rotation periods, is shown at the lower right of each panel in Fig. 3. Particle positions in each Poincaré section lie on a single Hamiltonian contour, confirming the flow's integrable character, although the evolution of the spatial distribution of points on the contour is not uniform. The theoretical prediction of the Brown–Samelson theorem, (that this flow, although complicated in physical space, is not chaotic) is confirmed.

4 Discussion

In this report we have extended the Brown–Samelson theorem to include baroclinicity through layered models. Specifically, particle motion arising from any flows given by Eq. (3) have a Hamiltonian and thus, according to that theorem, are integrable. We have illustrated the utility of the theorem by examining solutions to the two layer modon problem with discontinuities in the vorticity field. In physical space the solutions exhibit complicated trajectories that may even cross discontinuities in q_j. Such behavior is suggestive of chaotic behavior. However, the Brown–Samelson theorem ensures integrable particle motion provided that the H_j

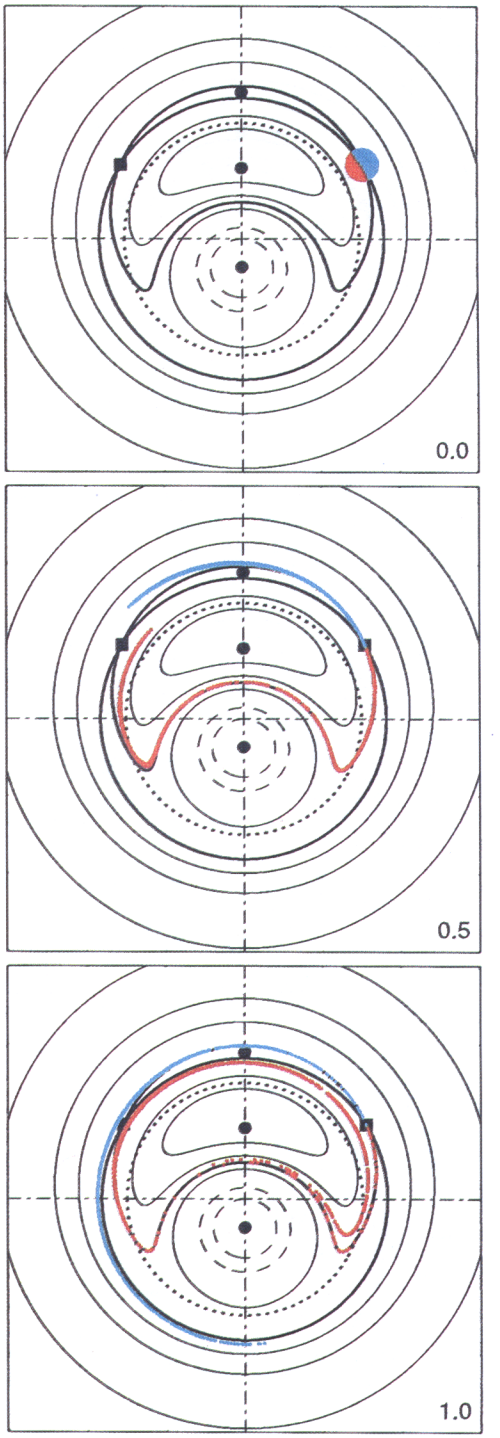

Fig. 2. Evolution of a circular blob of particles (initially positioned at the saddle point in the upper right quadrant) over one modon rotation. Particle positions are referenced to a frame that rotates with the modon and are overlaid on contours of the upper layer Hamiltonian, constructed in the same way as those in Fig. 1. Particles shown in red were initially positioned at a radius less than or equal to the saddle point radius. Particles shown in blue were initially positioned at a radius greater than the saddle point radius. Time (in modon periods) is shown at the lower right in each panel.

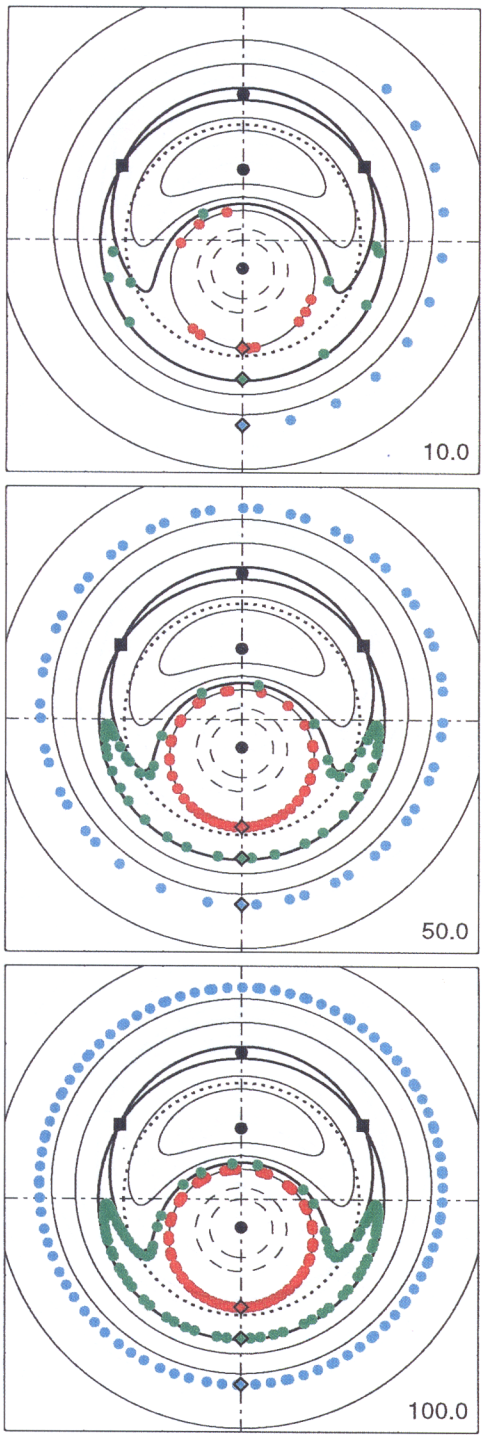

Fig. 3. Evolution of the Poincaré sections for the three particle trajectories shown in Fig. 1. The Poincaré sections are overlaid on contours of the upper layer Hamiltonian, constructed as in Fig. 1. Poincaré sections for the particle trajectory shown in the (upper, middle, lower) panel of Fig. 1 are shown in (red, green, blue). Time (in modon periods) is shown at the lower right in each panel.

generated from the system of Eq. (10) through Eq. (12) have a non–zero gradient everywhere or are within invariant submanifolds in which zero gradient points have been removed. Such points, when they occur, are the critical points of the canonical flow. Numerically generated Poincaré sections verify that particle motion follows level contours of H_j and hence are regular. It is disappointing to note, however, that some standard software packages for estimating Lyapunov exponents and fractal dimensions indicate the presence of chaos for this case. See Tsonis *et al.* (1994) for another caution regarding such estimates.

This study shows that the Brown–Samelson theorem may be useful for classifying nonsteady dynamically balanced baroclinic flows. It also suggests that chaotic behavior might be produced in the rotating modon model if perturbative forcing were applied. In the case considered here, the Brown–Samelson theorem provides both the justification and machinery for reducing this class of problems to an investigation of the geometric properties of the Hamiltonians.

Unanswered by this analysis is the possible introduction of non–integrability by allowing any of the twelve solution parameters (Table 1, for example) to vary with time. Since many of these parameters may be expected to vary with time, chaotic solutions for this class of motions are likely to exist in nature.

Acknowledgements. The authors are pleased to acknowledge the constructive criticisms and encouragement of M. Brown. Support from the Office of Naval Research is gratefully acknowledged as is the Samuel L. and Fay M. Slover endowment to Old Dominion University. The skills and patience of Carole E. Blett and Karal Gregory were most helpful for technical editing and formatting.

References

Brown, M. G., Phase space structure and fractal trajectories in 1 1/2 degree of freedom Hamiltonian systems whose time dependence is quasiperiodic, *Nonlin. Proc. Geophys.*, In press, 1998.

Brown, M. G. and Samelson, R. M., Particle motion in vorticity conserving two–dimensional incompressible flows, *Phys. Fluids, 6*, 2875-2876, 1994.

Dewar, W. K., Planetary shock waves, *J. Phys. Oceanogr., 17*, 470-482, 1987.

Dewar, W. K., Arrested fronts, *J. Mar. Res., 49*, 21-52, 1991.

Dewar, W. K., Spontaneous shocks, *J. Phys. Oceanogr., 22*, 505-522, 1992.

Flierl, G. R., Larichev, V. D., McWilliams, J. C. and Reznik, G. M., The dynamics of baroclinic and barotropic solitary eddies, *Dyn. Atmos. Oceans, 5*, 1-41, 1980.

Holdzkom, J. J. II, Hooker, S. B. and Kirwan, A. D., Jr., A comparison of a hydrodynamic lens model to observations of a warm–core ring, *J. Geophys. Res., 100*, 15,889-15,897, 1995.

Hooker, S. B., Brown, J. W. and Kirwan, A. D., Jr., Detecting "dipole ring" separatrices with zebra palettes, *IEEE Trans. Geosci. Rem. Sens., 33*, 1306-1312, 1995.

Joyce, T., Gulf stream warm–core ring collection: An introduction, *J. Geophys. Res., 90*, 8801-8802, 1985.

Joyce, T. M. and Kennelly, M. A., Upper–ocean velocity structure of Gulf Stream warm-core ring 82B, *J. Geophys. Res., 90*, 8839-8844, 1985.

Kirwan, A. D., Jr., R. P Mied, and B. L. Lipphardt, Jr. Rotating modons over isolated topography in a two–layer ocean. *ZAMP, 48*, 535–570, 1997.

Lipphardt, B. L., Jr., *Dynamics of dipoles in the Middle Atlantic Bight.* Dissertation, Old Dominion University, Norfolk, VA, 1995.

Mied, R. P., Kirwan, A. D., Jr. and Lindemann, G. J., Rotating modons over isolated topographic features, *J. Phys. Oceanogr., 22*, 1569-1582, 1992.

Nof, D., Geostrophic shock waves, *J. Phys. Oceanogr., 16*, 886-901, 1986.

Stern, M. E., Minimal properties of planetary eddies, *J. Mar. Res., 33*, 1-13, 1975.

Tsonis, A. A., Triantafyllou, G. N., Elsner, J. B., Holdzkom, J. J. II and Kirwan, A. D., Jr., An investigation of the ability of nonlinear methods to infer dynamics from observables, *Bull. Am. Met. Soc., 75*, 1623-1633, 1994.

Whitham, G. B., *Linear and Nonlinear Waves.* Wiley–Interscience, New York, 1974.